J Mater Sci: Mater Electron (2024) 35:1622

Interrogation of Sudan yellow dye imprints on L-Lysine Sulphate (SLLS) semiorganic crystalline form with the assistance of experimental and computational investigations for nonlinear optical applications

Pachaiyappan Sanjeevi[1], Logeswari Jayaseelan[2], Kamatchi Thennarasu[1], and Kumaresan Parasuraman[1,*]

[1] *Research Department of Physics, Thiru.A.Govindasamy Government Arts College, Tindivanam, Tamil Nadu 604 307, India*
[2] *Department of Chemistry, Marudhar Kesari Jain College for Women, Vaniyambadi, Tirupattur, Tamil Nadu 635 751, India*

Received: 18 May 2024
Accepted: 17 August 2024

ABSTRACT

The amino acid L lysine, with its unstable protonated α-amino group and deprotonated α-carboxylic acid group, can be mixed with diluted sulphuric acid to create the semiorganic crystal complex L-Lysine Sulphate (LLS). Sudan yellow, an azodye, was used to enhance LLS's chemical and physical properties. The study presents theoretical and experimental results on SLLS single crystals, which belong to the Orthorhombic system with the P_{21} space group. The Fourier transform infrared emission spectrum of a foundation crystalline form of SLLS was measured using various instruments. The spectrum showed a decrease in the NH^{3+} group's symmetry, increased N–H···O hydrogen bonding, and cationic dyes elongation. The lower local symmetry Carbons was present in the SO_4 structure, activating dormant IR modes and dividing degenerate IR modes. The optical absorption of SLLS was determined at 200–800 nm, with a wide absorption maximum in the intense ultraviolet area at around 280 nm. The electrophilicity index (ω) measures the energy reduction caused by the maximum flow of electrons across the source and acceptor. The study concludes that semiorganic crystal SLLS are well suited for nonlinear optical resonators (NLO) applications.

1 Introduction

The materials that exhibit a nonlinear behavior when exposed to a light source could potentially be categorized as nonlinear optical (NLO) materials. Technologies such as information technology and manufacturing sectors are significantly impacted by nonlinear optical (NLO) materials, which are important in the discipline of nonlinear optical technology. Over the past decade, this endeavor has yielded

Address correspondence to E-mail: logeshkumaresan@yahoo.com

https://doi.org/10.1007/s10854-024-13419-1
Published online: 23 August 2024

results in nonlinear optical applications. In essence, performance can be connected with the NLO elements' enhanced efficiency. The growing need for components for technological purposes has led to increased keen interest in a crystal's formation mechanism [1–3]. Semiorganic resources show possibilities in a variety of fields, including phase modulation, light amplitude, and optoelectronic equipment construction [4]. In the visible spectrum of electromagnetic radiation, the incorporation of substances that are inorganic and organic (semiorganic)results in a huge nonlinear optical (NLO) spectrum and great transparency in the visible spectrum. Extensive research has already been conducted on crystalline salts of amino acids that are optically active, including L arginine, L histidine, and L lysine [5]. The amino acid L lysine comprises two groups: the protonated α-amino group ($-NH_3^+$ form) and the deprotonated α-carboxylic acid group (-COO − form). There are hydrogen atoms in its side chain ($(CH_2)_4NH_2$). For the purpose of forming metal organic crystals, this side chain provides a charge transmission [6]. Under normal circumstances, it is very unstable [7]. Thus, the chemical configuration of L lysine needs to be changed through the addition of minerals in the form that comprise acids and bases in order to increase its stability. Sulfuric acid corrodes easily and is very reactive. It dissolves in both ethyl alcohol and water. When coupled with organic material (light paper or other flammable materials), its high reactivity might cause it to burn. L-Lysine is mixed with diluted sulphuric acid to generate the semiorganic crystal complex L-Lysine Sulphate (LLS). The chemicals known as azo dyes account for around half of the the globe's overall colorant output [8]. This dye family's major feature is the existence of the azo group (N = N-), which allows for more prolonged electronic conjugation of π electrons, resulting in high light absorption in the visible band of the spectrum of electromagnetic waves. Thus, Sudan yellow is an azodye that was used as a dopant in the current investigation in combination with L-Lysine Sulphate in order to enhance both its chemical and physical properties.

The work yields an optically active nonlinear single crystal Sudan yellow dye-doped L-Lysine Sulphate (SLLS). The theory and experimental results about Sudan yellow azodye's effects on crystal formation, FTIR, UV–VIS, FMO energies, the consequences Mulliken, whereas MESP have been implemented to measure electronic charges, and the quantum mechanical traits of SLLS single-crystal specimens are provided and discussed in the present article. Studies have shown that the dyes' filling of the crystal vacancies is what gives SLLS crystals their enhanced characteristics. By doing this, the crystal structure is optimized and its imperfections are decreased. Furthermore, interactions between doped molecules and crystal hosts help to enhance the electrical and optical characteristics of SLLS crystals.

2 Experimental details

Fine AR standard l-lysine salts have been introduced to a 1:1 acetone and water mixture, in addition to the same volume of sulfuric acid. A constant stirring and mild heating were applied to the LLS solution. In accordance with the solubility molar proportion, the Sudan yellow dye was subsequently added. The mother solution is used to suspend a certain number of small, ideal, and highly observable crystals of seed which are formed by spontaneous nucleation process. For the purpose of producing LLS at more advanced factors, sudan yellow supplemented salt solution had initially been synthesized by successive recrystallization. Using the method of slow evaporation solution synthesis approach under ambient temperature, single crystals of SLLS were produced from a completely saturated solution of the synthetic salt of LLS. In the saturated solution form, spontaneously occurring grain nucleation yielded crystalline forms featuring a desirable morphology without minimal macrodefects. Following within thirty days, outstanding optical quality crystals with dimensions of up to $8 \times 7 \times 5$ mm^3 were formed. Figure 1 depicts pictures of as-grown SLLS crystals.

2.1 Computational technique

The computer program Gaussian 09 W was used to perform the quantum chemicals characterization using the B3LYP approach, implementing the LANL2DZ basis set. Multiwfn [9] was used to make mapping pictures of RDG, as well as to analyze the electrical wave functions.

3 Results and discussions

3.1 Single crystal X-ray diffraction analysis

To study the X-ray diffraction of the SLLS crystal, an ENRAF NONIUS CAD 14 automatic mode X-Ray diffractometer was implemented. The crystal's lattice parameters are $a = 5.74$ Å, $b = 10.39$ Å,

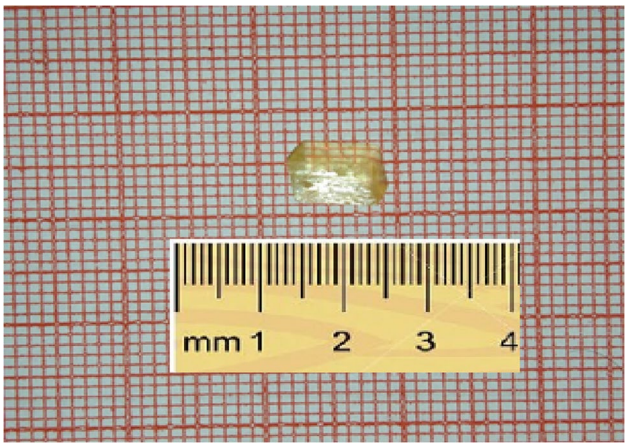

Fig. 1 A captured image of a grown SLLS crystal

$c = 15.69$ Å,, $\alpha = \beta = \gamma = 90°$, indicating it is associated within the Orthorhombic system that belongs to the P21 space group, according to the data in Table 1 which agrees with the earlier findings.

3.2 FTIR measurements

By employing a PerkinElmer Spectral RX1 spectroscope paired implementing a $LiTaO_3$ sensors, KBr ray splitting device, and He–Ne beams applying lasers reliable sources, the Fourier transform infrared radiation emission spectra of the a foundation crystalline form have been measured in the 400–4000 cm^{-1} wavelength range of values. Using KBr, SLLS was compressed onto a solid pellet shape for forming the material to be investigated.

Figure 2 shows the resulting spectrum. All of these different modes are IR activated. The NH_3^+ group's asymmetric vibrations are responsible for the faint band seen at 3363 cm^{-1} in the FTIR. In FTIR, the symmetric stretching vibrations appear as a medium band at 3159 cm^{-1}. Due to hydrogen bonds between molecules incorporating a total of three of this amino group's N–H bands that are present, the vibration associated with stretching exhibits a lower wave number. The splitting of the degenerate mode and the emergence of a medium band at 2681 cm^{-1} indicate that the NH_3^+ group's symmetry is decreased in SLLS. Increased N–H···O bonding to hydrogen will yield dyes with cationic molecules portion of the compound elongating because of the transfer of charges from the electron isolated pairs. The initially observed elongation action is swiftly succeeded by the cation's structural disruption, which causes a corresponding the blue shift occurs corresponding to the N–H stretching wave number is additionally visible.

The lysine residues' electrical environment is altered by the in-phase translocation caused by three atoms of hydrogen of NH_3^+. The lower local symmetry Carbons is present in the SO_4 that is shown in the LLS structure. The dormant IR modes are activated and the degenerate IR modes divide as a result of this symmetry lowering. Bands are detected at 1462, 1404, 1203, and 1080 cm^{-1}. In the solid state, this supports the symmetry lowering of SO_4. This shows quite clearly that the $(SO_4)^{2-}$ ion in this crystal does not have perfect symmetry. Computed FTIR of SLLS was shown in Fig. 3.

3.3 UV–VIS measurements

The Perkin Elmer LAMBDA 950 UV–VIS-NIR Spectrophotometer was used to examine the SLLS crystal's UV–Vis-NIR spectra in the 190–1100 nm wavelength range. UV–Vis spectral analysis was used to determine the optical absorption of SLLS at 200–800 nm, as shown in Fig. 4. As can be seen from the picture, the sample appears to have a wide

Table 1 SXRD parameters of SLLS

Parameters	LLS [10]	ALLS [previous work]	SLLS [present work]
Crystal structure	Orthorhombic	Orthorhombic	Orthorhombic
Space group	P_{212121}	P_{212121}	P_{212121}
Cell parameters			
a	5.573 Å	6.735 Å	5.74 Å
b	11.536 Å	15.945 Å	10.39 Å
c	16.594 Å	12.365 Å	15.69 Å
$\alpha = \beta = \gamma$	90°	90°	90°
Volume	1066.8304 ($Å^3$)	1108.4568 ($Å^3$)	1008.8692 ($Å^3$)
Crystal size	12 mm × 11 mm × 5 mm	20 mm × 7 mm × 16 mm	8 mm × 7 mm × 5 mm

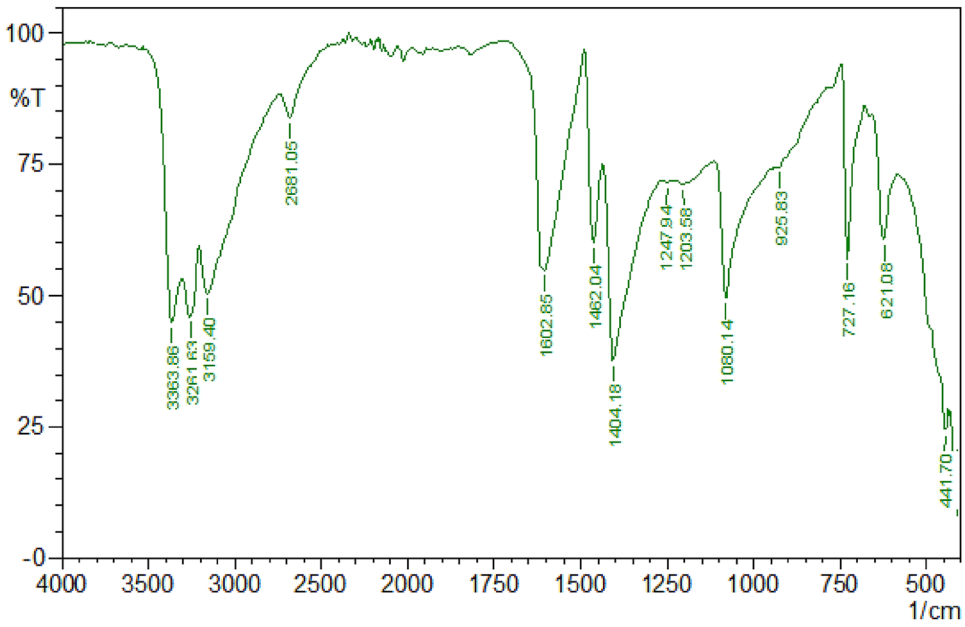

Fig. 2 Experimental FTIR spectrum of the SLLS molecule

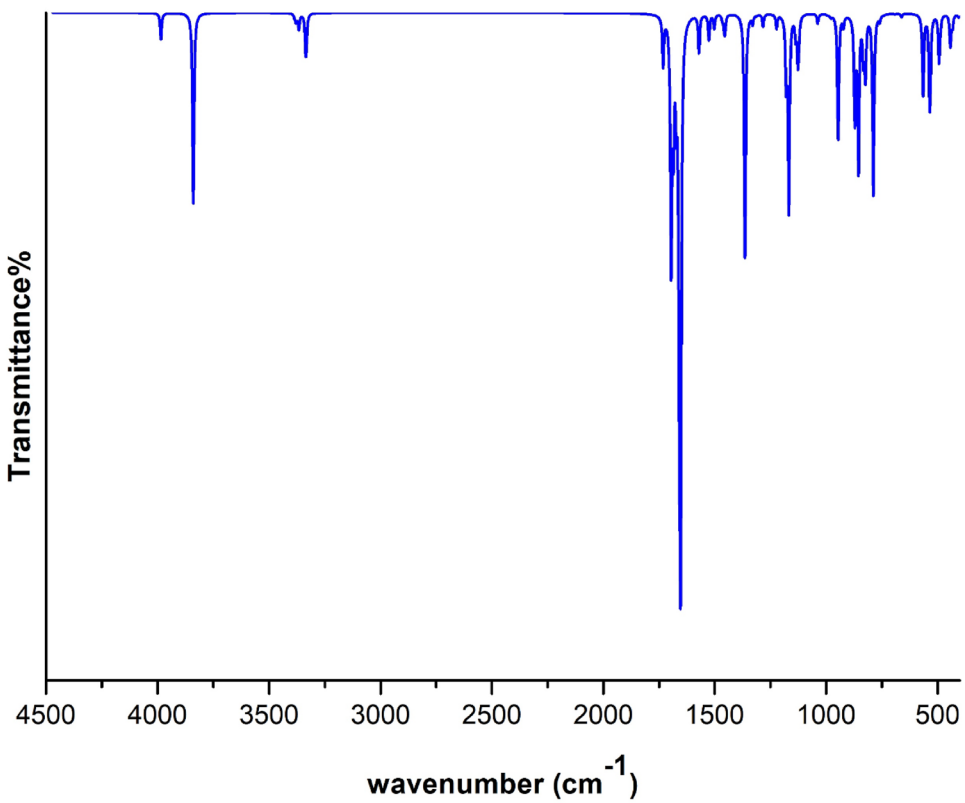

Fig. 3 Theoretical FTIR spectrum of the SLLS molecule

absorption maximum in the intense ultraviolet area at around 280 nm. The mentioned samples have an optical band gap of 3.86 eV. A computational framework in the fields of physics and astronomy called Time-Dependent Density Functional Theory (TDDFT) combines the considerably more complicated N-body wavefunction with the time-dependent electron concentration as the primary factor,

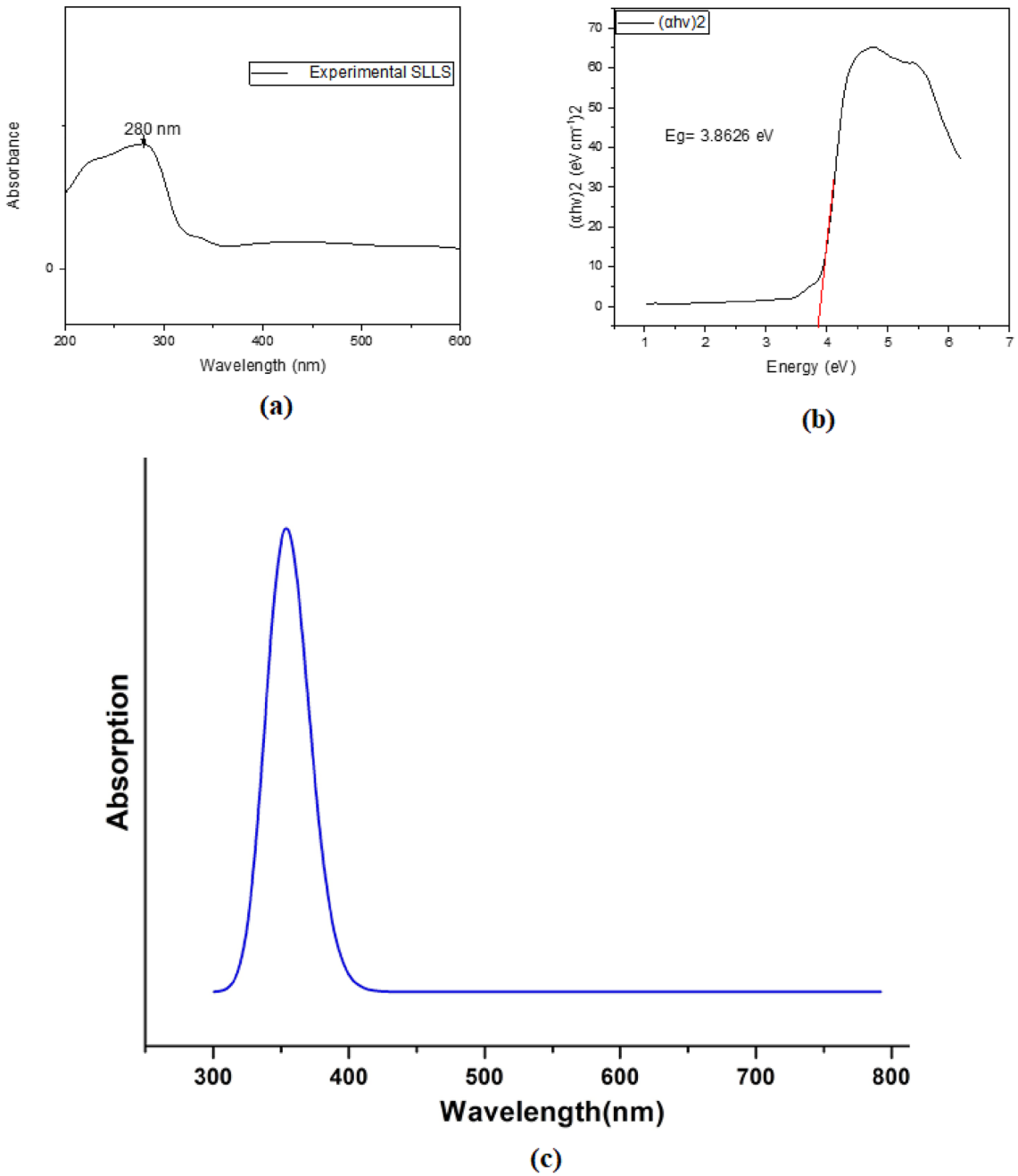

Fig. 4 **a**, **b**, **c** Experimental and Computational UV–Vis spectrum of the SLLS molecule

simplifying the conceptualization of a system [11]. The TD-DFT approach is used to generate theoretical UV–Vis spectra for the TD B3LYP/ LANL2DZ level in the gas phase. The calculated wavelength is 262 nm, 353 nm, 542 nm while the experimental wavelength is 280 nm. The findings of the experiment and computation agree pretty closely. The calculated parameters are implemented, along with the oscillator strength ($f = 0.0049$) and frequencies. The parameters are tabulated in Table 2.

3.4 HOMO–LUMO evaluation

The HOMO–LUMO gap and first hyper polarizability possess a reciprocal correlation within the first hyper polarizability significance, enabling the orbitals of the

molecules to cross each other and ensure appropriate electronic communication the conjugation process. This serves as an indicator of the intramolecular transfer of charges regarding the particle's electron donating group towards the electron accepting group by means of the p-conjugation manner [12]. The technique of vibration spectroscopy has been applied to investigate several organic compounds possessing conjugated p-electrons that have high molecular first hyperpolarizabilities [13]. On the other hand, intramolecular transfer of charges between the donor towards acceptor groups across a single-double bond conjugated channel-related may trigger substantial modifications in the polarizing capacity and molecular moment of dipole within a the molecule itself. The frontier molecular orbitals, also known as HOMO and LUMO, are the most significant orbitals in a molecule. Interactions between the molecule and other individuals are determined by these orbitals. The frontier orbital gaps can explain the compound's mechanical the strength as well as its biochemical reactive properties. Small frontier orbital gaps are related with higher polarizability, low kinetic stability, and strong chemical reactivity. These molecules are also known as soft molecules. Frontier molecular orbitals have a critical influence in the electric and optical characteristics of moleculesSmall divergence exists between the highest occupied molecular orbital and lowest unoccupied molecular orbital (HOMO–LUMO) in molecules that are conjugated because of significant intramolecular charge movement that occurs from end-capping electron-donor pairs towards the enforceable electron-acceptor groups by means of the p-conjugated method [13]. The HOMO denotes having the capacity to provide an electron, versus the LUMO that is, meaning electron recipient, denotes the capacity to accept an electron from a source. The B3LYP/6-311G++(d,p) technique calculates the HOMO and LUMO energies, which are illustrated below.

The difference in energy across HOMO and LUMO is shown in Table 3, suggesting that charge transfer about Sudan yellow doped with LLS components as Fig. 5 might have been taking place. The energy difference between the HOMO and LUMO orbitals, known as the energy gap, is an important quantity for evaluating molecule electrical transport parameters and measuring electron conductivity. Local and global chemical reactivity descriptors of compounds, including softness, hardness, chemical potential, electronegativity, and electrophilicity index, have been established based on density functional descriptors. Pauling's theory started out defining electronegativity as a particle's ability to attract electrons within a complicated system. The

Table 3 The HOMO–LUMO gap of energy together with the molecular characteristics of SLLS

Molecular properties	B3LYP/6–311++G(d,p)
HOMO	$-7.5558\ eV$
LUMO	$-2.0700\ eV$
LUMO—HOMO (Energy gap)	$9.6258\ eV$
Global hardness (η)	$-2.2974\ eV$
Electronegativity (χ)	$-4.9812\ eV$
Global softness (s)	$-269.5494\ eV$
Chemical potential (μ)	$4.9812\ eV$
Global Electrophilicity (ω)	$-4.5222\ eV$
Dipole moment (μ)	2.0966 Debye
Mean polarizability(α)	-67.9480×10^{-30} esu
Anisotropy of the polarizability ($\Delta\alpha$)	598.3190×10^{-30} esu
First hyperpolarizability(β)	1.421×10^{-30} esu
Optimized global minimum Energy	−853. 1295(Hartrees)

Table 2 Calculated at B3LYP / LANL2DZ basis set, estimated wavelength, energy, oscillator strength, including substantial contribution from SLLS

Compound	Method	Solvent	Wavelength (nm)	Band gap (eV)	Energy (cm^{-1})	Oscillator strength	Symmetry	Major contributions
SLLS	DFT	Gas	542	2.3	18,462	0.0	Singlet-A	H-1->LUMO (89%) H-1->L+2 (4%)
			353	3.5	28,291	1.1819	Singlet-A	HOMO->LUMO (95%)
			262	4.7	38,207	0.0049	Singlet-A	H-2->LUMO (47%), HOMO->L+4 (31%)
	Expt	-	280	3.8	–	–	–	–

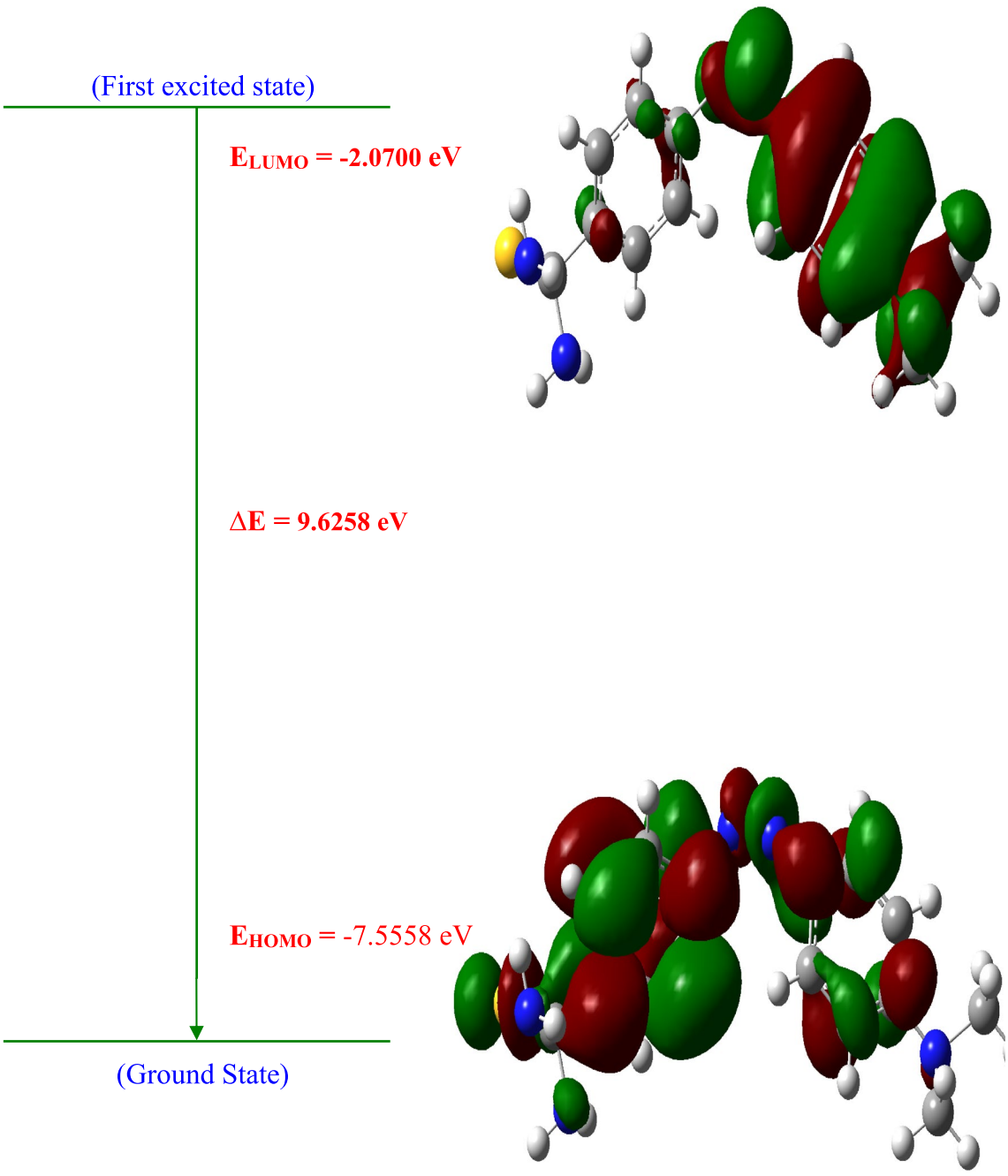

Fig. 5 HOMO–LUMO Visualization of the Sudan yellow doped LLS

following are the definitions of softness, electronegativity (χ), chemical potential (μ), and hardness (η).

$$\eta = 12\partial^2 E \partial N^2(r) = 12\partial\mu\partial N v(r),$$

$$\mu = \partial E \partial N v(r),$$

$$\chi = -\mu = -\partial E \partial N v(r),$$

where E represents an N-electron system's electronic energy and v(r) represents its external potential. Compound softness is a property that indicates the level of a substance's interaction. It indicates a reverse of the level of hardness.

$S = 1\eta.$

Relating Koopman's theory to closed-shell complexes

$$\mu = -(1 + A)^2,$$

$$\chi = (1 + A)^2,$$

where as A and I stand for the components' corresponding electron affinities along with ionization potentials. The capacity of a compound to receive exactly a single electron from a source that donates is known as electron affinity. Conversely, fractional transfer of charges happens in many different kinds of bonds, including covalent bonds with hydrogen. Parr et al. [14] developed the electrophilicity index (ω) to assess a compound's global electrophilic character. The electrophilicity coefficient (ω), as established by Parr et al. [14], is an indicator to measure the energy reduction brought about by the maximum flow of electrons across the source of electrons and acceptor. The electrophilicity index (ω) was defined by them in the following way.

$\omega = \mu^2 2\eta.$

Incorporating this just obtained reactivity value which was recently proved in comprehending the toxicity of different contaminants by means of their chemical reactivity in order along with sites specificity. The biochemical activity of sudan yellow doped with LLS is described by the computed electrophilicity index significance. Table 3 presents the results of all the computations for the electrophilicity index, potential, softness, and hardness.

3.5 Mulliken population analysis

The subsequent table displays the overall atomic charges of sudan yellow doped with LLS as determined by Mulliken's population analysis with B3LYP in various basis sets. It is evident from the outcome that the aromatic ring's substitution of CH3 atoms causes an electron density redistribution [14, 15]. The reduction in electron density demonstrates the hydrogen atom's σ-electron absorbing properties in SLLS. Nearly comparable atomic charges are present in the CH3 group. According to the Mulliken charge derived from the 6–311++G(d,p)basis set, the atoms C1, C3, C4, H7, H8, H9, H10, H12, H13, H15, H17, H18, and H20 have greater positive charge, making them more acidic values are given in Table 4. Figure 6 illustrates the Mulliken plot of SLLS crystals.

3.6 Magnetic susceptibility

Natural paramagnetic behavior is exhibited by every material with a persistent moment of magnetization. Given a magnetic field, paramagnetic materials tend to align itself with the field's orientation, producing positive susceptibility to magnetic attraction that is temperature-dependent. This is because thermal agitation will cause the dipoles of magnetic materials to shift away from synchronization. Table 5 shows the anticipated magnetic susceptibility (χm) of molecules at different temperatures using unpaired electrons [15, 16]. This table depicts the relationship between (χm) and 1/T ($temperature^{-1}$). It is discovered that the effective magnetic moment is a constant, 1.7063×10^{-5} (BM), is the numerical value that represents the Curie constant, which is 3.39174×10^{-5}, is derived from the magnetic moment (μm).

3.7 Molecular electrostaticpotential (MESP)

For the SLLS molecule that exists, the MESP plots its molecular size, form, and electrical energy values concurrently. MESP mappings has become extremely beneficial for studying the link between the structure of molecules and physiological chemical characteristics. The red-colored MESP about sudan yellow doped with LLS readily demonstrates each of the three primary electron-rich zones surrounding the nitrogen atoms, whereas the blue-colored region indicates the region containing the entirety of the atoms of hydrogen carries the majority of the charge that is positive. Somewhere between the extremes of bright red and deep blue colors in Fig. 7, the green-colored area on the MESP surface correlates to an electrical potential.

3.8 Thermodynamic properties

The quantitatively thermodynamics values for the SLLS molecule were determined using the mathematical frequencies of harmonics based on vibrational measurements investigation. Table 6 summarizes the results of the calculation findings, focusing on entropy ($Sm\ o$), heat capacity (Cp), and enthalpy variations ($\Delta Hm\ o$). Several thermodynamic

Table 4 The assessed Mulliken in addition to natural atomic energies of SLLS

Atoms	Mulliken	Natural
C1	−0.30516	−0.12246
C2	−0.11319	−0.38683
C3	−0.18386	−0.19585
C4	−0.15742	−0.35980
C5	−0.17830	−0.19156
C6	−0.16709	−0.36806
H7	−0.10687	−0.19557
H8	−0.17714	−0.39749
H9	−0.11546	−0.40353
H10	−0.15848	−0.38450
H11	0.18354	0.47619
H12	−0.27510	−0.15703
C13	−0.03731	−0.20032
C14	−0.08930	−0.19379
C15	−0.08825	−0.19015
C16	−0.09061	−0.19088
H17	0.00349	−0.18819
C18	0.13225	0.17239
C19	−0.28929	−0.54877
C20	0.21418	0.19917
H21	0.20525	0.11196
H22	0.19528	0.13029
N23	0.19528	0.11389
C24	0.20494	0.10853
H25	0.19539	0.10837
H26	0.19587	0.11429
H27	0.20563	0.10945
C28	0.20573	0.10922
H29	0.20291	0.11494
H30	0.20968	0.12682
H31	0.20515	0.12396
C32	0.19657	0.13526
S33	0.19509	0.12706
N34	0.21006	0.11121
N35	0.20309	0.10804
H36	0.20194	0.10570
H37	0.21184	0.19179
H38	0.25205	0.16119
H39	0.15298	0.10329

coefficients increase with temperature within the region of 100 to 1000 K, as the data in Table 6 demonstrates, with the remarkable exemption about Gibb's free energy [17]. The reason for this occurs due to the fact that when temperature increases, molecular vibrational intensities increased. Quadratic formulae were used to fit the linear correlation relationships between Gibb's energy encompasses free form, ambient temperature, entropy, deviations in enthalpy, followed by heat capacity; Considering every single of the aforementioned thermodynamics capabilities, the corresponding a correlation coefficient factors (R^2) are, in that order, 0.996; additionally 0.9997, and 0.9995. The associated combining equations are as follows, with relationship graphs displayed in Fig. 8.

$$Cp, o = -.0244 + 0.12021 + 9.5247 \times ?10?^{(-5)}T^2 (R^2 = 0.9996)$$

$$Sm\, o = -5.2741 + 0.1544T + 52.0862 (R^2 = 0.9997)$$

$$\Delta Hmo = 3.2610 + 0.0192T - 2.4532 (R^2 = 0.9995)$$

Regarding the purpose of further researching the sudan yellow doped with LLS, all of the thermodynamic data provide useful information. These are presented in Table 6 and may be utilized for predicting chemical reactions pathways predicated upon the thermodynamics second terms of principle, computational harmonics frequency ranges, with the purpose of estimating additional performances thermodynamics energy based on associations between thermodynamic variables.

3.9 The RDG analysis

To comprehend the mechanism of interactions among molecules of organic matter and inorganic metallic compounds, RDG analysis is being carried out. The RDG is a technique for assessing noncovalent relationships in a chemical system as well as estimating specific weak connections, including Van Der Waals and hydrogen bonding relationships and also the steric influences [18, 19]. Figure 9 depicts RDG graphs made using the Multiwfn 3.8 software package. The molecular structure depicted in Fig. 9 has three color emits: green, red, and blue. The three colors are linked to the van der Waals, steric effect (repulsive), together with H-bond relationships, in each case. The repulsive relationship (red loop) is found within organic unit atomic particles, which have a strong steric influence. The relationship between Sudan yellow, L-lysine, and sulfate is determined to have the strongest van der Wall interaction (shown in green).

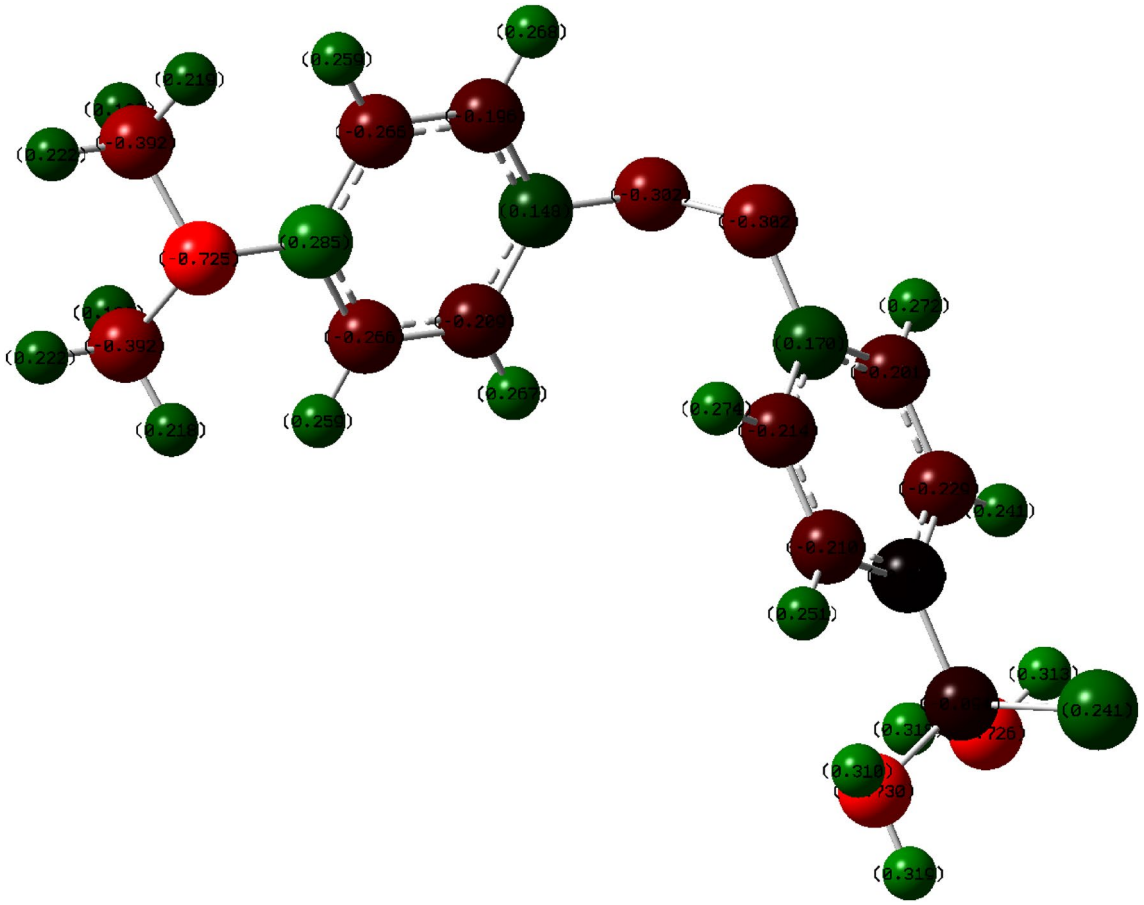

Fig. 6 Plot of Mulliken's atomic charges of sudan yellow doped with LLS

Table 5 Magnetic susceptibility of Sudan yellow doped with LLS by B3LYP/6–311++G (d, p)

Temperature (°C)	Magnetic susceptibility	1/Susceptibility	1/Temperature
50	1.01752E-06	982,779.7335	0.02
100	5.08761E-07	1,965,559.467	0.01
150	3.39174E-07	2,948,339.201	0.006667
200	2.54381E-07	3,931,118.934	0.005
250	2.03504E-07	4,913,898.668	0.004
273	1.86359E-07	5,365,977.345	0.003663
298.15	1.70639E-07	5,860,315.551	0.003354
300	1.69587E-07	5,896,678.401	0.003333
350	1.4536E-07	6,879,458.135	0.002857
400	1.2719E-07	7,862,237.868	0.0025
450	1.13058E-07	8,845,017.602	0.002222
500	1.01752E-07	9,827,797.335	0.002

4 Conclusion

Nonlinear optical materials (NLO) exhibit nonlinear behavior when exposed to light, impacting technologies like information technology and manufacturing. Semiorganic resources show potential in various fields, including phase modulation, light amplitude, and optoelectronic equipment

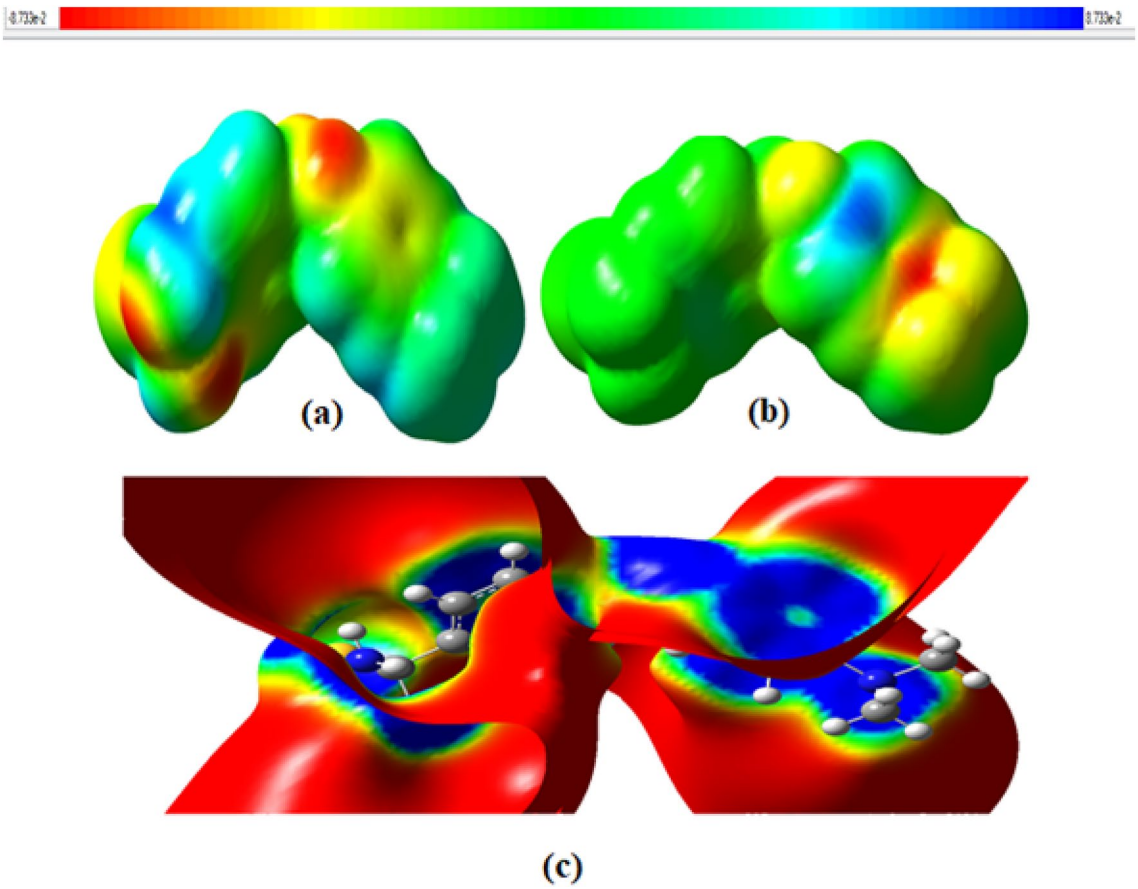

Fig. 7 **a, b, c** The contour representations of electrostatic potential for both the positive and negative potentials in SLLS

construction. Sudan yellow, an azodye, was used as a dopant to enhance its chemical and physical properties. The study focuses on the characterization of quantum chemicals using the B3LYP approach, implementing the LANL2DZ basis set. The crystal's lattice parameters indicate it belongs to the Orthorhombic system with the P_{21} space group. FTIR measurements show that the NH_3^+ group's symmetry decreases in the crystal SLLS, and increased N–H···O hydrogen bonding results in the cationic dyes portion of the compound elongating due to the transfer of charges from electron isolated pairs. The study examines the chemistry and toxicity of Sudan yellow doped with LLS crystals, revealing that the (SO4)2 – ion in the crystal does not have perfect symmetry. The biochemical activity of sudan yellow doped with LLS is described by the computed electrophilicity index significance. Thermodynamic properties for the SLLS molecule were determined using mathematical frequencies of harmonics based on vibrational measurements. Thus, the study concludes that semiorganic crystal SLLS are well suited for NLO applications.

Table 6 The thermodynamic characteristics of sudan yellow treated with LLS as obtained by the DFT/B3LYP 6–311++G(d,p) technique are influenced by temperature

T(K)	S ($J.mol^{-1}.K^{-1}$)	Cp ($J.mol^{-1}.K^{-1}$)	ΔH0 → T ($kJ.mol^{-1}$)
100	72.04588906	18.61615678	1.3026
200	87.92065004	28.14053536	3.6472
298.15	100.8867112	37.45697895	6.8642
300	101.1185468	37.63145313	6.9336
400	113.2146271	46.73757167	11.1616
500	124.5124282	54.56261947	16.2380
600	135.045411	60.94168257	22.0244
700	144.8398661	66.09464623	28.3843
800	153.9483747	70.29397701	35.2127
900	162.4354684	73.75717013	42.4187
1000	170.3585085	76.64674948	49.9450

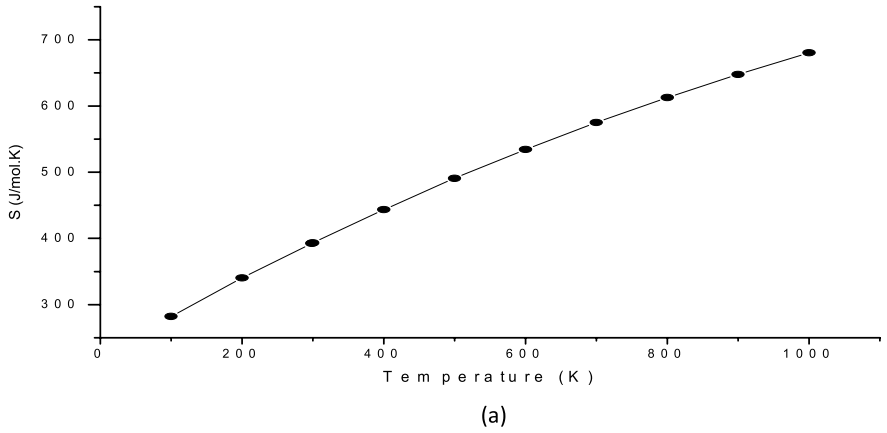

(a)

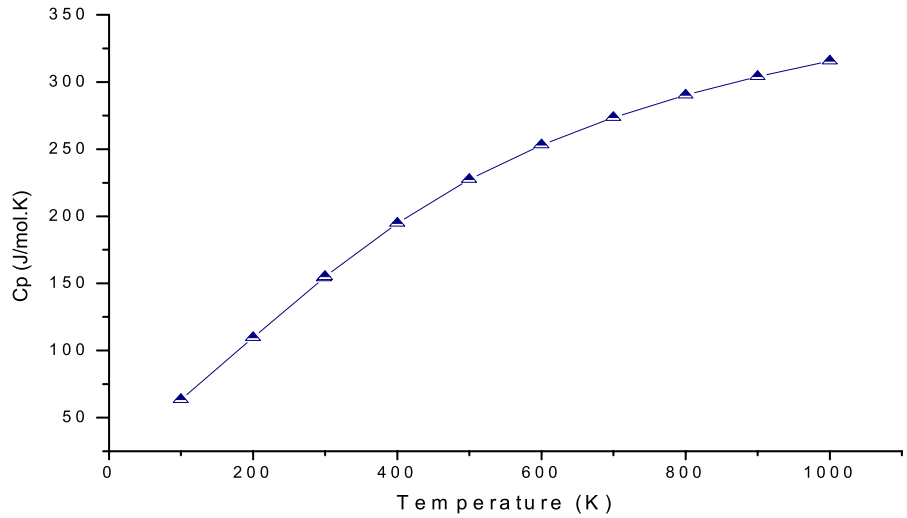

(b)

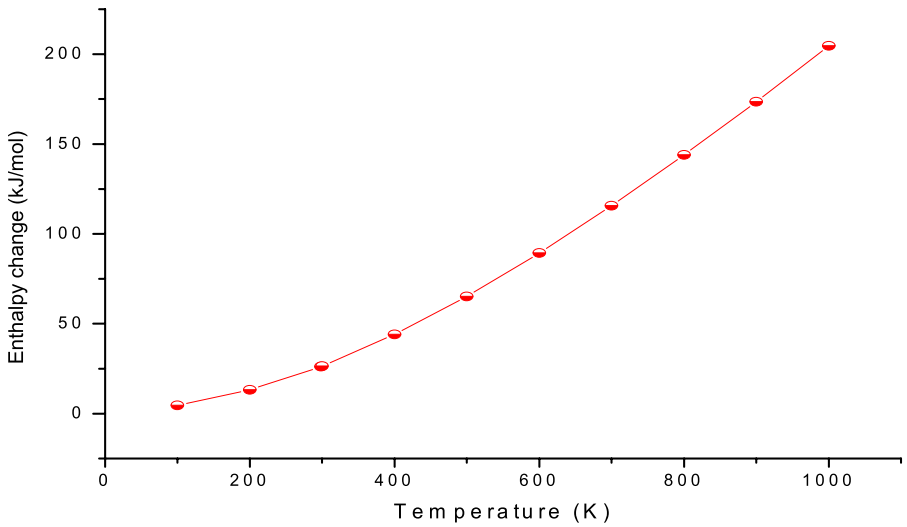

(c)

Fig. 8 **a, b, c** The effect of temperature on entropy (S), heat capacity (C_p) & enthalpy change ($\Delta H0 \rightarrow T$) of SLLS

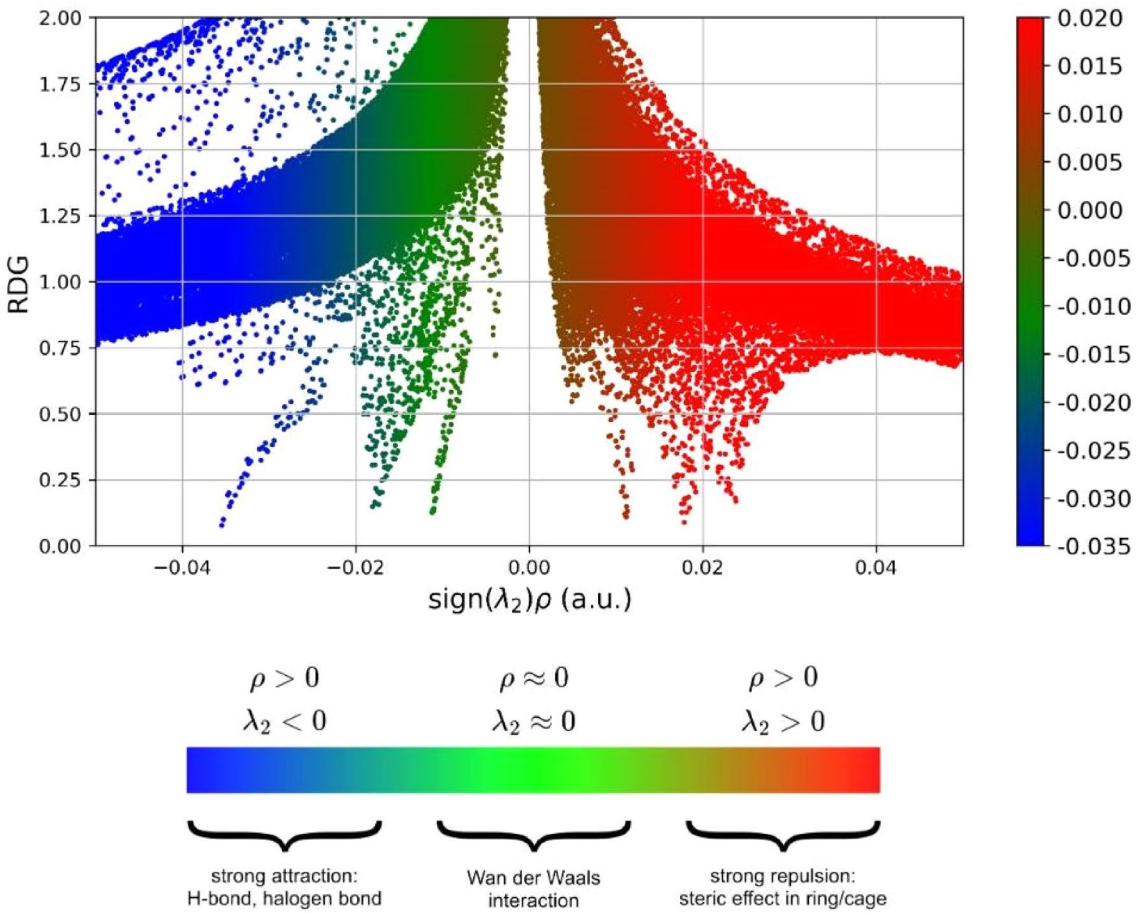

Fig. 9 RDG graphs created with the Multiwfn of SLLS crystal

Author contributions

Pachaiyappan S—Writing, software and visualizations. Logeswari J—Resources, software and revising. Kamatchi T—Review and editing, Methodology. Kumaresan P- Supervision, Validation and funding acquisition.

Funding

The authors have not disclosed any funding

Declarations

Conflict of interest The authors have no competing interests to declare that are relevant to the content of this article.

Informed consent Informed consent was obtained from all individual participants included in the study.

Research involving human and animal rights There is no Human participants and/or Animals involved in the research.

References

1. R.A. Laudise, R. Ueda, J.B. Millin, *Crystal Growth and Characterization* (North-Holland Publishing Co, Amsterdam, 1975)
2. J.C. Brice, *Crystal Growth Processes* (Halsted Press, Hoboken, 1986)
3. H.S. Nalwa, S. Miyata, *Nonlinear Optics of Organic Molecules and Polymers* (CRC Press Inc, Boca Raton, 1996)
4. G. Marudhu, S. Krishnan, T. Thilak, P. Samuel, G. Vinitha, G. Pasupathi et al., Thermal and mechanical studies on

nonlinear optical material diglycine barium chloride monohydrate (DGBCM) single crystal. J. Nonlinear Opt. Phys. Mater. **22**(4), 1350043 (2013)
5. V. Vasudevan, R. Ramesh Babu, A. Reicher Nelcy, G.G. Bhagavannarayana, K. Ramamurthy, Synthesis, growth, optical, mechanical and electrical properties of L-lysine L-lysinium dichloride nitrate (L-LLDN) single crystal. Bull. Mater. Sci. **34**(3), 469 (2011)
6. R.N. Shaikh, M. Anis, M.D. Shirsat, S.S. Hussaini, Investigation on the linear and nonlinear optical properties of L-lysine doped ammonium dihydrogen phosphate crystal for NLO applications. IOSR-JAP **6**(1), 42 (2014)
7. M. Tao, M. Zhu, W. Chunnuan, Z. He, Degradation kinetic study of lysine in lysine hydrochloride solutions for injection by determining its main degradation product. Asian J. Pharmacol. Sci. **10**(1), 57 (2015)
8. D.B. MacDougall, *In Colour in Food-Improving Quality, 21* (Woodhead Publishing Limited and CRC Press, Cambridge, 2002)
9. J.I. Aihara, J. Phys. Chem. A **103**, 748 (1999)
10. V. Krishnakumar, S. Manohar, R. Nagalakshmi, Semiorganic nonlinear optical l-lysine sulphate growth and characterization. Spectrochim. Acta Part A: Mol. Biomol. Spectrosc. **75**, 1394–1397 (2010). https://doi.org/10.1016/j.saa.2009.12.081
11. F. Calvayrac, P.-G. Reinhard, E. Suraud, C.A. Ullrich, Nonlinear electron dynamics in metal clusters. Phys. Rep. **337**(6), 493–578 (2000)
12. K. Sambathkumar, S. Jeyavijayan, M. Arivazhagan, Electronic structure investtigations of 4-aminophthal hydrazide by UV–visible, NMR spectral studies and HOMO–LUMO analysis by ab initio and DFT calculations Spectrochim. Acta A **147**, 51–66 (2015)
13. K. Sambathkumar, Vibrational spectra, NBO, HOMO–LUMO and conformational stability studies of 4-hydroxythiobenzamideSpectrochim. Acta A **147**, 51–66 (2015)
14. B. Latha, P. Kumaresan, S. Nithiyanantham, K. Sambathkumar, J. Mol. Struct. **1142**, 255–260 (2017)
15. K. Sambathkumar, S. Nithiyanantham, Synthesis, characterization and theoretical properties of coumarin NLO single crystal by DFT method. J. Mater. Sci.: Mater. Electron. **28**, 6529–6543 (2017)
16. G. Suresh, K. Sahadevan, K. Sambathkumar, P. Kumaresana, Indian J. Pure Appl. Phys. **57**, 196–204 (2019)
17. K. Sambathkumar, 2014 Density functional theory studies of vibrational spectra, Homo- Lumo, Nbo and Nlo analysis of some cyclic and heterocyclic compounds (Ph.D thesis). Bharathidasan University, Tiruchirappalli.
18. O. Noureddine, N. Issaoui, M. Medimagh, O. Al-Dossary, H. Marouani, Quantum chemical studies on molecular structure, AIM, ELF, RDG and antiviral activities of hybrid hydroxychloroquine in the treatment of COVID-19: Molecular docking and DFT calculations. J. King Saud Univ. Sci. **33**(2), 101334 (2021). https://doi.org/10.1016/j.jksus.2020.10133420
19. A. Sagaama, N. Issaoui, O. Al-Dossary, A.S. Kazachenko, M.J. Wojcik, Non covalent interactions and molecular docking studies on morphine compound. J. King Saud Univ. Sci. **33**(8), 101606 (2021). https://doi.org/10.1016/j.jksus.2021.101606